Steep waves in free-surface flow past narrow topography

Stephen L. Wade,[1] Benjamin J. Binder,[1,a)] Trent W. Mattner,[1] and James P. Denier[2]
[1]*School of Mathematical Sciences, The University of Adelaide, Adelaide, Australia*
[2]*Department of Mathematics, Macquarie University, Sydney, Australia*

(Received 3 February 2017; accepted 1 June 2017; published online 21 June 2017)

In this work, we compute steep forced solitary wave solutions for the problem of free-surface flow over a localised topographic disturbance in an otherwise flat horizontal channel bottom. A single forced solitary wave and a double-crested forced solitary wave solution are shown to exist, both of which approach the Stokes limiting configuration of an included angle of 120° and a stagnation point at the wave crests. The solution space for the topographically forced problem is compared to that found in Wade *et al.* ["On the free-surface flow of very steep forced solitary waves," J. Fluid Mech. **739**, 1–21 (2014)], who considered forcing due to a localised distribution of pressure applied to the free surface. The main feature that differentiates the two types of forcing is an additional solution that exists in the pressure-forced problem, a steep wave with a cusp at a single wave crest. Our numerical results suggest that this cusped-wave solution does not exist in the topographically forced problem. *Published by AIP Publishing.* [http://dx.doi.org/10.1063/1.4986262]

I. INTRODUCTION

The steady unforced solitary wave is well-known and has been widely studied, with particular interest having been paid to the nonlinear phenomena. The study of the steady steep waves has found evidence of connections between these phenomena to wave breaking in an unsteady flow, a real-world example being given by ocean waves breaking near the shore. An early discovery was that the highest wave has a sharp crest with a 120° included angle and stagnation point known as a Stokes limiting configuration.[1–3] It was later determined that for steady unforced solitary waves, the highest wave is not the fastest, and the height of the wave is not unique with respect to the wave's speed and energy as the highest wave is approached.[4–13] A remarkable connection exists between an instability found at the crest of the unforced solitary wave, which is a localised phenomenon, and the turning points of the wave-energy with respect to the wave's mean height, which is a global quantity.[14–16]

More recently, Wade *et al.*[4] established that the non-unique behaviour of the steady almost-highest unforced wave is also found when the free surface is forced by a localised pressure disturbance of amplitude A. In the aforementioned work, five basic types of steady solutions were investigated for two-dimensional supercritical flows, with a depth-based Froude number of $F > 1$ (see Fig. 1). Following the enumeration scheme of Wade *et al.*, single-crested waves are identified as type-I and type-II solutions, and these are classified as perturbations to a uniform stream and solitary wave, respectively. A cusped single-crested wave is identified as a solution of type III, and like the type-II solution, it is a perturbation to a single solitary wave. A double-crested wave is identified as a type-IV solution and is classified as a perturbation to two solitary waves separated by a uniform stream. The type-V solution is characterised by a single wave trough (lower than the height of the uniform flow far upstream and downstream of the disturbance) and is classified as a perturbation to a uniform stream. Wade *et al.* showed that the solution types II–IV all appear to approach the Stokes-limiting configuration with stagnation points at the wave crests.

In this paper, we consider forcing due to a localised topographical disturbance in the otherwise flat horizontal bottom of a channel. The forcing is a bump for amplitude $A > 0$ or a trench for amplitude $A < 0$ (see Fig. 2). In moderate flow regimes, the basic solution types I–V have been shown to exist in the nonlinear steady flow problem.[17–21] However, the existence and non-uniqueness of the solution types II–IV that approach the Stokes limiting configuration have not been confirmed in the case of topographic forcing.

We exploit a modified version of the numerical method developed in Wade *et al.*[4] to investigate the topographically forced flow. We show that the flow-types II and IV approach the Stokes-limiting configuration with stagnation points at the crests, similar to that found in the pressure forced flow problem. However, we find no almost-highest type-III solutions with the numerical method, leaving open the question of whether cusp wave crest-solutions for the Stokes limiting configuration exist in the topographically forced flow. The diminishing effect of the channel topography on the free surface as the depth of a trench is increased is another difference from the negatively pressure forced system. This disparity between the flow due to pressure forcing on the free surface and that of topographical forcing is summarised illustratively with plots of the mid-stream free-surface elevation versus the amplitude of forcing.

II. FORMULATION

We consider steady two-dimensional irrotational flow of an incompressible and inviscid fluid of uniform density. The

a)Electronic mail: benjamin.binder@adelaide.edu.au

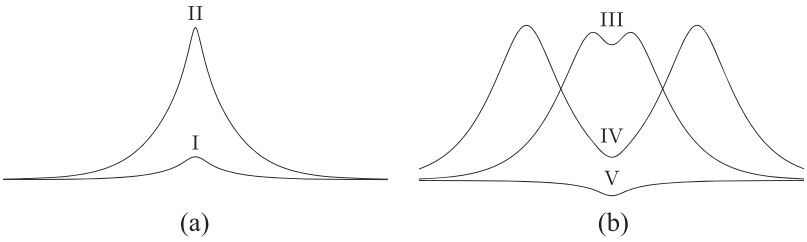

FIG. 1. Sketch of the five basic types of solutions for localised forcing due to either a distribution of pressure on the free surface or a topographical disturbance on the bottom of the channel, $F > 1$. (a) Forcing with $A > 0$ and (b) $A < 0$.

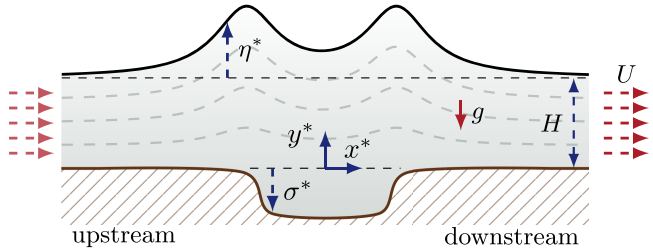

FIG. 2. Schematic of the steady flow problem. The free surface is denoted by $y^* = H + \eta^*$. The topography, $y = \sigma^*$, is stationary with respect to the wave crest(s).

flow domain is bounded above by the free surface $y^* = H + \eta^*$ and below by the impermeable topography of the channel $y^* = \sigma^*$. A Cartesian coordinate system (x^*, y^*) is chosen as shown in Fig. 2. The only body force on the fluid is gravity, g, which acts in the negative y^* direction. It is assumed that the topography and the flow are symmetric about the y^* axis. As $|x^*| \to \infty$, the flow approaches a uniform supercritical stream of constant depth H and speed U. The Froude number of the flow is

$$F = \frac{U}{\sqrt{gH}} > 1.$$

The depth and speed of the uniform stream in the far field are used to define the non-dimensional quantities

$$(x, y, \eta, \sigma) = (x^*, y^*, \eta^*, \sigma^*)/H \quad \text{and} \quad (u, v) = (u^*, v^*)/U, \tag{1}$$

where u^* and v^* are the horizontal and vertical components of the velocity, respectively, which satisfy

$$u \to 1, \quad v \to 0, \quad \eta \to 0, \quad \sigma \to 0 \quad \text{as} \quad |x| \to \infty. \tag{2}$$

The dynamic and kinematic boundary conditions are Bernoulli's equation and a no-penetration condition, respectively,[22] expressed in these non-dimensional quantities as the equations

$$\frac{1}{2}(u^2 + v^2) + \frac{y}{F^2} = \frac{1}{2} + \frac{1}{F^2} \quad \text{on} \quad y = 1 + \eta \tag{3}$$

and

$$u\eta_x = v \quad \text{on} \quad y = 1 + \eta \quad \text{and} \quad u\sigma_x = v \quad \text{on} \quad y = \sigma, \tag{4}$$

respectively. The system is closed with the imposition of conservation of mass for an incompressible fluid

$$u_x + v_y = 0 \quad \text{for} \quad \sigma < y < 1 + \eta. \tag{5}$$

The solution for the unknown free-surface elevation, η, is determined by solving (5) subject to (2)–(4). This is done by introducing the velocity potential ϕ and streamfunction ψ for the flow. Without loss of generality, we set $\psi = 1$ on the free surface, and it follows that $\psi = 0$ on the bottom of the channel. We set $\phi = 0$ at $x = 0$. The numerical solution for η is then computed using a boundary-integral method,[4,23–25] which only involves unknown quantities on the streamlines $\psi = 0$ and $\psi = 1$. Comprehensive details on the numerical method, which we used to find solutions, can be found in the work of Wade.[26]

With this method, the dimensionless quantities (1) are given parametrically in terms of ϕ and ψ; therefore, we prescribe the topography parametrically as

$$\sigma(\phi) = \frac{\hat{A}}{2}\left(\tanh 10(\phi + \phi_\mathrm{i}) - \tanh 10(\phi - \phi_\mathrm{i})\right) \quad \text{on} \quad \psi = 0, \tag{6}$$

where ϕ_i is the location of the downstream inflexion point of the topography. The topography in the physical coordinates (x, y) is not given explicitly by the above formula; after obtaining the solution to the free surface, we numerically evaluate $x(\phi)$ and $y(\phi)$ by integrating the identity $\mathrm{d}(\phi + \mathrm{i}\psi)/\mathrm{d}(x + \mathrm{i}y) = 1/(u - \mathrm{i}v)$. The constant 10 in (6) was chosen to ensure that bumps and trenches had a smooth box-like appearance as in Fig. 2. The inflection points are chosen to be located one non-dimensional unit of distance apart; therefore,

$$x(\pm\phi_\mathrm{i}) = \pm 1/2 \quad \text{on} \quad \psi = 0. \tag{7}$$

The amplitude of forcing is defined as

$$A = \int_{-\infty}^{\infty} \sigma(\phi)\,\mathrm{d}\phi,$$

whose absolute value is the area of the disturbance. The sign of A indicates whether the forcing is a bump or a trench (see Fig. 2).

III. RESULTS

We begin our discussion with the general layout of the results shown in Figs. 3 and 4, where we plot the mid-stream free-surface elevation, $\eta(0)$, versus the amplitude of forcing, A. In each panel, the solid curves are for a fixed value of the Froude number, which is systematically incremented in (a)–(d). The broken curves are for almost-highest waves, where the flow is approaching the Stokes limiting configuration at the wave crests, with variable Froude number. Markers indicate the location in the parameter space of the five basic types of solution and some of the almost-highest waves.

The results in Fig. 3 are for a localised topographical disturbance on the bottom of channel, described by Eqs. (6) and (7). These are to be compared to the results in Fig. 4

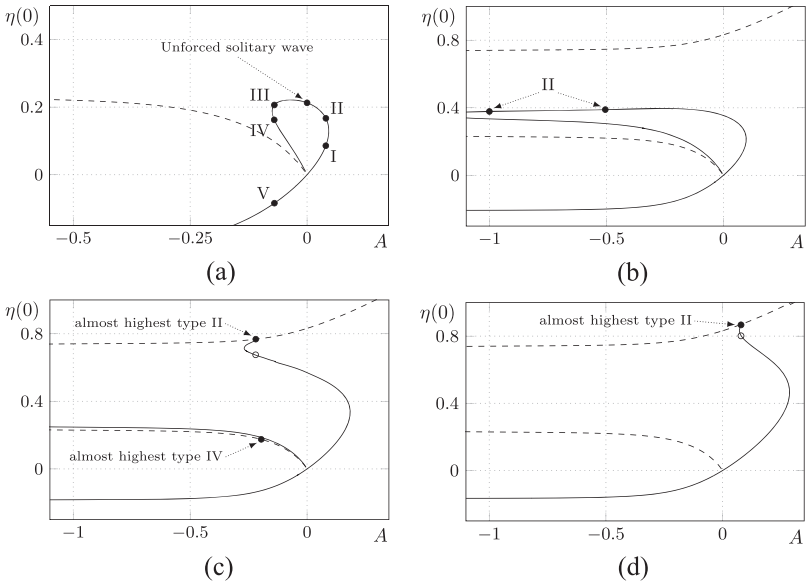

FIG. 3. The case of topographical forcing. Plots of the mid-stream free-surface elevation, $\eta(0)$, versus the amplitude of forcing, A. The solid curves in each panel (a)–(d) are for a fixed value of the Froude number, $F = \{1.10, 1.16, 1.24, 1.32\}$. The broken curves are for the loci of the almost-highest waves, with $|u| = 0.03$ fixed at the wave crests and variable Froude number. The markers in (a) indicate the location in the parameter space of the unforced solution and the five basic types of forced solution, whereas in (b), they identify the waves in Fig. 5, and in (c) and (d), they identify the almost-highest waves in Figs. 6–8.

[Reproduced with permission from Wade *et al.*, "On the free-surface flow of very steep forced solitary waves," J. Fluid. Mech. **739**, 1–21 (2014). Copyright 2013 Cambridge University Press] which are for a localised pressure distribution on the free surface. For both types of forcing, a qualitatively similar parameter space is observed for the smallest value of the Froude number in panel (a) of each figure (solid curves). This is not surprising as this result is well-known in the nonlinear problem, and it is also found analytically in the weakly nonlinear approximation of the problem[4,17–21] (and others). However, there is a striking difference between the results for the two types of forcing, as the Froude number is increased in panels (b)–(d) of Figs. 3 and 4. The most noticeable difference is that we find no type-III almost-highest wave solutions in the case of topographical forcing, where the upper and lower broken curves in Fig. 3 represent almost-highest wave type-II and type-IV solutions, respectively.

The disparity between the results for the two types of forcing is mainly due to the diminishing impact that the depth of the trench (i.e., when $A < 0$) has on the free-surface profile in the topographically forced case. This is illustrated for two type-II solutions with markers in Fig. 3(b) and their corresponding streamlines in Fig. 5. The majority of streamlines from each solution (broken and solid curves) are nearly coincident in Fig. 5, despite the difference in the trench's depth. This diminishing influence of the trench's depth on the free-surface profile is also observed for the almost-highest type-II and type-IV solutions, and the type-V solutions, where the two broken curves and lower solid curve all appear to approach horizontal asymptotes as $A \to -\infty$ in Figs. 3(b)–3(d). This limiting behaviour, as $A \to -\infty$, is not observed in the pressure forced problem (see Fig. 4).

Having shown, at least within the constraints of the numerical method of Wade *et al.*,[4] that the almost-highest type-III solutions may not exist in the topographically forced problem, we now turn our attention to the almost-highest type-II and type-IV solutions. To facilitate discussion of the almost-highest waves, we introduce the wave crest-height

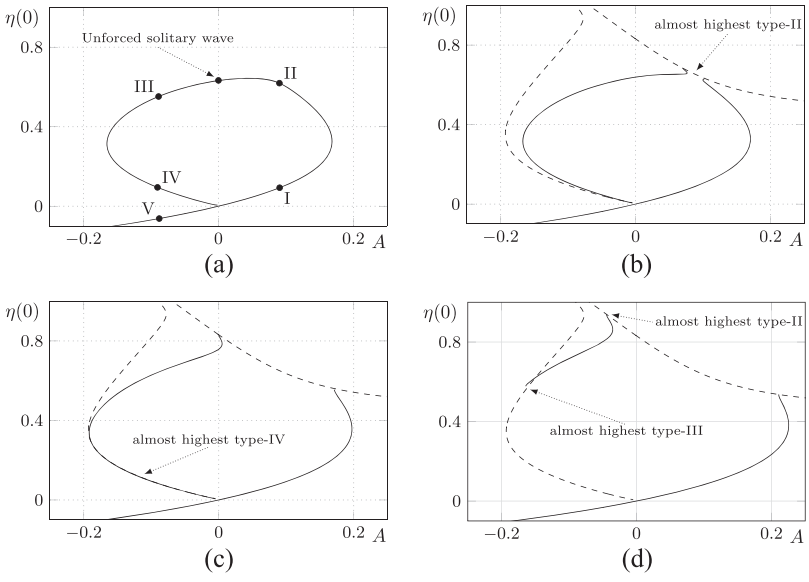

FIG. 4. Pressure forcing [Reprinted with permission from Wade *et al.*, "On the free-surface flow of very steep forced solitary waves," J. Fluid. Mech. **739**, 1–21 (2014). Copyright 2013 Cambridge University Press]. Plots of the mid-stream free-surface elevation, $\eta(0)$, versus the amplitude of forcing, A. The solid curves in each panel (a)–(d) are for a fixed value of the Froude number, $F = \{1.26, 1.262, 1.2909, 1.32\}$. The broken curves are for the loci of the almost-highest waves, with $|u| = 0.05$ fixed at the wave crests and variable Froude number. The markers in (a) indicate the location in the parameter space of the unforced solution and the five basic types of forced solution.

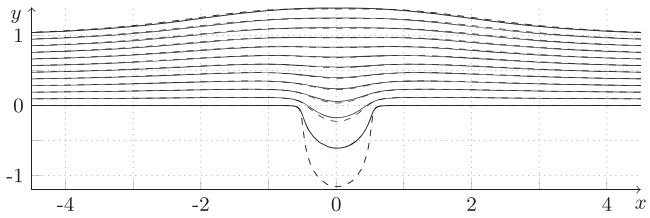

FIG. 5. Streamlines for two type-II solutions with $F = 1.16$. Solid curves, $A = -0.5$; broken curves, $A = -1.0$.

parameter

$$\omega = 1 - (u_c F)^2,$$

as defined by Longuet-Higgins and Fox[7] and others, where u_c is the horizontal component of the velocity at the location of a wave crest. This parameter represents a rescaled wave height, with a maximum value of $\omega = 1$.

We begin by examining two almost-highest type-II solutions with the same value of $F = 1.24$ and $A = -0.22$. The solutions are indicated by the open and solid markers closest to the upper broken curve in Fig. 3(c) for values of $\omega = 0.813$ and $\omega = 0.990$, respectively. The streamlines for both solutions are given in Fig. 6. This demonstrates the non-uniqueness of almost-highest type-II solutions for the flow past a trench, with the taller wave [upper solid marker in Fig. 3(c) and solid curves in Fig. 6, $\omega = 0.990$] approaching the Stokes limiting configuration of an included angle of 120° at the wave crest. Similar sets of results are found for the almost-highest type-IV solutions with $A < 0$ [single solid marker closest to the lower broken curve in Fig. 3(c) and curves in Fig. 7] and the almost-highest type-II solutions with $A > 0$ [markers in Fig. 3(d) and curves in Fig. 8(a)].

Further examination of the non-unique behaviour of the almost-highest waves is exemplified with type-II solutions for fixed $A = 0.079$ in Fig. 8(b), where we plot the variation in F for given values of ω. The location of the two profiles from panel (a) is shown by the solid and open markers indicating taller ($\omega = 0.993$) and shorter ($\omega = 0.862$) waves, respectively, as in Fig. 3(d). Two turning points, one local maxima at $\omega = 0.923$ and one local minima at $\omega = 0.996$, are seen as $\omega \to 1$. These plots then serve to demonstrate that the tallest wave is not the fastest. Additional turning points may be calculated (decreasing in amplitude) with further grid refinement in the numerical method, and we expect that there are infinitely many turning points as $\omega \to 1$, as conjectured in the unforced problem.[8,10]

To demonstrate the non-unique behaviour of another global, integral, quantity of the flow, we examine the mass

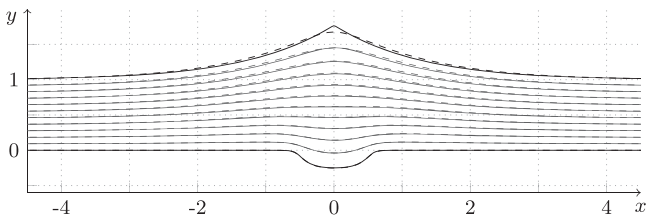

FIG. 6. Streamlines for two almost-highest type-II solutions with $F = 1.24$ and $A = -0.22$. Broken curves, $\omega = 0.813$; solid curves, $\omega = 0.990$.

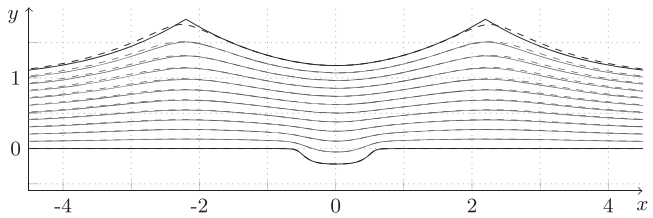

FIG. 7. Streamlines for two almost-highest type-IV solutions with $F = 1.2906$ and $A = -0.196$. Broken curves, $\omega = 0.813$; solid curves, $\omega = 0.990$.

of the wave

$$m = \int_{-\infty}^{\infty} y(\phi) \frac{\mathrm{d}x}{\mathrm{d}\phi} \, \mathrm{d}\phi \quad \text{on} \quad \psi = 1.$$

In Fig. 8(c), we plot m versus ω for type-II solutions with fixed $A = 0.079$ and observe an oscillatory behaviour similar to that shown in Fig. 8(b). The local maximum of m occurs at $\omega = 0.837$ and the local minimum at $\omega = 0.993$. The most massive wave is thus shorter than the fastest wave, the wave with greatest Froude number, for the flow over a bump of fixed size. The oscillatory behaviour in Figs. 8(b) and 8(c) is also found for almost-highest waves with a trench (type-II and type-IV, $A < 0$), and this result has previously been shown in the unforced[8,10] and pressure-forced[4] problems.

We now turn our attention to a discussion of the variation of F along the solution branches corresponding to the almost-highest wave (broken curves) in Fig. 3, with reference to the value of the Froude number for the highest unforced solitary wave

$$F_u = 1.2909,$$

as calculated by Williams[13] and others. First, we consider the almost-highest type-II solutions for a flow past a trench (upper broken branch in Fig. 3, $A < 0$). The upper branch emanates from the $A = 0$ axis with $F = F_u$ (i.e., the highest unforced solitary wave), and the value of F decreases as the branch is followed into the $A < 0$ half-plane. We obtained converged solutions up to a value of $A = -1.1$ with a corresponding value of $F = 1.22$ but remark that the branch is likely to extend beyond this point, potentially towards a horizontal asymptote at $F \approx 1.22$. In the case of almost-highest type-II waves for the flow past a bump, we follow the branch that emanates from the unforced highest solitary wave solution into $A > 0$ half-plane. In our computations, F appears to increase along this branch in an unbounded manner. Therefore, we expect the almost-highest waves with a bump to exist for all $F > F_u$.

In contrast, the variation in F is very small for the almost-highest type-IV solutions (the lower broken branch in Fig. 3 with $A < 0$) when compared to that of the type-II solutions. Along this branch, the value $F \approx F_u$. This is because the two crests are at some distance from the trench, and so each crest is locally similar to the limiting configuration of an unforced highest solitary wave. A similar result is found in the case of pressure-forced almost-highest type-IV solutions. For both types of localised forcing, the type-IV solutions do not exist for values for $F \geq F_u$ [see solid curves emanating from the origin into the second quadrant of the $(A, \eta(0))$-plane in Figs. 3 and 4].

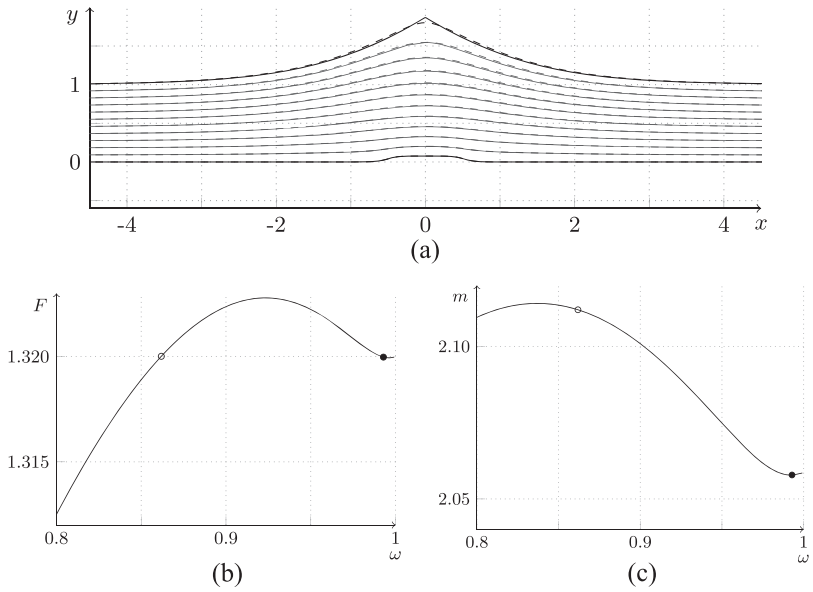

FIG. 8. Analysis of almost-highest type-II solutions with $A = 0.079$. (a) Streamlines for two almost-highest type-II solutions with $F = 1.32$. Broken curves, $\omega = 0.862$; solid curves, $\omega = 0.993$. [(b) and (c)] Plots of the Froude number F and wave mass m versus ω. The markers indicate the location of the solutions shown in (a).

IV. CONCLUDING REMARKS

We have considered the almost-highest forced solitary waves for free-surface flow over a localised topographic disturbance in an otherwise flat horizontal channel bottom. Modifying and implementing the numerical method of Wade *et al.*,[4] we computed solutions for localised topography of unit width. Only two types of almost-highest waves were found to exist, a single forced solitary wave and a double-crested forced solitary wave. Both types of solution were shown to approach the Stokes limiting configuration of an included angle of 120° and a stagnation point at the wave crests, exhibiting the same oscillatory and non-unique behaviour of that found in the unforced[8,10] and pressure-forced[4] problems.

We find no evidence of almost-highest waves with a cusp at a single wave crest in the topographically forced problem, which have previously been shown to exist in the pressure-forced problem.[4] This is a significant difference in the solutions for the two types of forcing, a previously unknown result, which we attribute to the diminishing influence of increasing the trench depth in the topographically forced case. Of course, and in theory, further exploration into the solution space, as $A \to -\infty$ (see Fig. 3), might confirm the existence of almost-highest cusped-wave solutions, or alternatively, as we suspect, they may simply not exist.

Finally, we remark that results for disturbances of comparable width are expected to be qualitatively similar to those presented and discussed in this work. This is commonly found in studies on steady two-dimensional free-surface flows where the qualitative behaviour is independent of the precise details of the disturbances (see references and cited papers therein). More specifically, Binder *et al.*[21] computed nonlinear type I–V solutions for rectangular disturbances with approximate widths of 0.5 and 10 non-dimensional units (see Figs. 3, 6, 12, and 13 in Ref. 21). However, wide disturbances do allow for additional types of solutions, including solutions with trapped periodic waves (see Figs. 13 and 14 in Ref. 21). The investigation of trapped almost-highest periodic waves with wave crests that approach the Stokes limiting configuration is left to future research.

[1] G. G. Stokes, *On the Theory of Oscillatory Waves* (Transactions Cambridge Philosophical Society, 1847), Vol. 8, pp. 441–455.
[2] G. G. Stokes, *Supplement to a Paper on the Theory of Oscillatory Waves*, Mathematical and Physical Papers (Cambridge University Press, 1880), Vol. 1, pp. 225–228.
[3] J. B. McLeod, "The Stokes and Krasovskii conjectures for the wave of greatest height," Stud. Appl. Math. **98**, 311–333 (1997).
[4] S. L. Wade, B. J. Binder, T. W. Mattner, and J. P. Denier, "On the free-surface flow of very steep forced solitary waves," J. Fluid Mech. **739**, 1–21 (2014).
[5] J. G. B. Byatt-Smith and M. S. Longuet-Higgins, "On the speed and profile of steep solitary waves," Proc. R. Soc. London, Ser. A **350**, 175–189 (1976).
[6] J. K. Hunter and J.-M. Vanden-Broeck, "Accurate computations for steep solitary waves," J. Fluid Mech. **136**, 63–71 (1983).
[7] M. S. Longuet-Higgins and M. J. H. Fox, "Theory of the almost-highest wave: The inner solution," J. Fluid Mech. **80**, 721–741 (1977).
[8] M. S. Longuet-Higgins and M. J. H. Fox, "Asymptotic theory for the almost-highest solitary wave," J. Fluid Mech. **317**, 1–19 (1996).
[9] M. S. Longuet-Higgins and J. D. Fenton, "On the mass, momentum, energy and circulation of a solitary wave. II," Proc. R. Soc. London, Ser. A **340**, 471–493 (1974).
[10] D. V. Maklakov, "Almost-highest gravity waves on water of finite depth," Eur. J. Appl. Math. **13**, 67–93 (2002).
[11] L. W. Schwartz and J. D. Fenton, "Strongly nonlinear waves," Annu. Rev. Fluid Mech. **14**, 39–60 (1982).
[12] J.-M. Vanden-Broeck, "Steep gravity waves: Havelock's method revisited," Phys. Fluids **29**, 3084–3085 (1986).
[13] J. M. Williams, "Limiting gravity waves in water of finite depth," Philos. Trans. R. Soc. London, Ser A **302**, 139–188 (1981).
[14] M. Tanaka, "The stability of solitary waves," Phys. Fluids **29**, 650 (1986).
[15] M. S. Longuet-Higgins and M. Tanaka, "On the crest instabilities of steep surface waves," J. Fluid Mech. **336**, 51–68 (1997).
[16] T. Kataoka, "The superharmonic instability of finite-amplitude interfacial waves," Fluid Dyn. Res. **38**, 831–867 (2006).
[17] L. K. Forbes and L. W. Schwartz, "Free-surface flow over a semicircular obstruction," J. Fluid Mech. **114**, 299–314 (1982).
[18] J.-M. Vanden-Broeck, "Free surface flow over an obstruction in a channel," Phys. Fluids **30**, 2315–2317 (1987).
[19] F. Dias and J.-M. Vanden-Broeck, "Open channel flows with submerged obstructions," J. Fluid Mech. **206**, 155–170 (1989).
[20] F. Dias and J.-M. Vanden-Broeck, "Generalised critical free-surface flows," J. Eng. Math. **42**, 291–301 (2002).

[21]B. J. Binder, F. Dias, and J.-M. Vanden-Broeck, "Influence of rapid changes in a channel bottom on free-surface flows," IMA J. Appl. Math. **73**, 254–273 (2007).
[22]H. Lamb, *Hydrodynamics* (Cambridge University Press, 1932).
[23]B. J. Binder and J.-M. Vanden-Broeck, "The effect of disturbances on the flows under a sluice gate and past an inclined plate," J. Fluid Mech. **576**, 475–490 (2007).
[24]C. J. Lustri, S. W. McCue, and B. J. Binder, "Free surface flow past topography: A beyond-all-orders approach," Eur. J. Appl. Math. **23**, 441–467 (2012).
[25]J.-M. Vanden-Broeck, "Numerical calculations of the free-surface flow under a sluice gate," J. Fluid Mech. **330**, 339–347 (1997).
[26]S. Wade, "Very steep solitary waves in two-dimensional free surface flow," Ph.D. thesis, The University of Adelaide, 2015.